

Efficient tensor networks for control-enhanced quantum metrology

Qiushi Liu and Yuxiang Yang

QICI Quantum Information and Computation Initiative, Department of Computer Science, School of Computing and Data Science, The University of Hong Kong, Pokfulam Road, Hong Kong, China

Optimized quantum control can enhance the performance and noise resilience of quantum metrology. However, the optimization quickly becomes intractable when multiple control operations are applied sequentially. In this work, we propose efficient tensor network algorithms for optimizing strategies of quantum metrology enhanced by a long sequence of control operations. Our approach covers a general and practical scenario where the experimenter applies $N-1$ interleaved control operations between N queries of the channel to estimate and uses no or bounded ancilla. Tailored to different experimental capabilities, these control operations can be generic quantum channels or variational unitary gates. Numerical experiments show that our algorithm has a good performance in optimizing the metrological strategy for as many as $N=100$ queries. In particular, our algorithm identifies a strategy that can outperform the state-of-the-art strategy when N is finite but large.

1 Introduction

Quantum metrology [1, 2, 3] can boost the precision of parameter estimation by exploiting quantum resources. Identification of optimal strategies for large-scale quantum metrology, however, is a daunting task suffering from the curse of dimensionality. Such challenges, for example, arise in estimating physical parameters encoded in many-body quantum systems [4, 5, 6, 7, 8] or many queries to an unknown quantum channel

[9, 10, 11, 12, 13, 14, 15]. In this work we focus on the quantum channel estimation problem.

It is a long-standing problem that, given N queries to a quantum channel \mathcal{E}_θ carrying the parameter of interest θ , what is the ultimate precision limit for estimating θ and how one could identify the optimal strategy that achieves the highest precision. For single-parameter estimation, precision bounds attainable by quantum error correction (QEC) [16, 17, 14] are known in the asymptotic limit ($N \rightarrow \infty$) and numerical algorithms for optimal strategies [18, 19] have been designed for small N (e.g., $N \leq 5$). These results, however, are under the assumption that unbounded ancilla is available. Meanwhile, little is known about the metrological performance for a large but finite N . On the other hand, in real-world experiments, quantum channel estimation for larger N with no or limited ancilla (for example, $N=8$ in Ref. [20]) can be demonstrated with identical-control-enhanced sequential use of quantum channels [20, 21]. Obviously, a gap exists between the theoretical results and the experimental requirement. The reason is that we lack an efficient way to tackle such problems for large N .

A fruitful approach to the classical optimization for large-scale quantum problems, mainly in many-body physics, is the tensor network formalism [22, 23]. Tensor networks provide an efficient way to classically store, manipulate and extract certain relevant information of quantum systems with limited many-body entanglement. In particular, this formalism has been used in quantum metrology for many-body systems to optimize the estimation precision and the corresponding input probe state [6].

It is natural to ask whether tensor networks can be used for optimizing a sequential strategy, where N channels can be applied one after an-

Qiushi Liu: qsliu@cs.hku.hk

Yuxiang Yang: yuxiang@cs.hku.hk

other, with interleaved control operations. This is possible by our intuition, as the power of tensor networks for addressing the spatial complexity is similarly applicable for handling the temporal complexity. For example, tensor networks have been used for quantum process tomography [24] and machine learning of non-Markovian processes [25].

In this work, we develop an efficient tensor network approach to optimizing control-enhanced sequential strategies for quantum channel estimation with bounded memory (see Fig. 1). Tailored to the experimental capability and programmability of quantum sensors, we design various algorithms based on tensor networks, for applying control operations that are either allowed to be arbitrary or restricted to identical quantum channels. Furthermore, by combining the tensor network with a variational circuit ansatz, we also cover the scenario where the control operations are restricted to unitary channels specified by possibly different or identical variational parameters. Formulating the problem fully within the matrix product operator (MPO) formalism, we apply the alternating optimization iteratively. The computational complexity for each round of the optimization is $O(N)$, where the input state and the $N - 1$ control operations are updated in each round. Our approach can efficiently optimize the estimation of qubit channels for $N = 100$, and outperform the state-of-the-art asymptotically optimal QEC approach [16, 17, 14] for finite N .

2 Framework

We start with some notations. We denote by $\mathcal{L}(\mathcal{H})$ the set of linear operators on a finite-dimensional Hilbert space \mathcal{H} , and $\mathcal{L}[\mathcal{L}(\mathcal{H}_1), \mathcal{L}(\mathcal{H}_2)]$ is the set of linear maps from $\mathcal{L}(\mathcal{H}_1)$ to $\mathcal{L}(\mathcal{H}_2)$. For a positive semidefinite operator A , we simply write $A \geq 0$.

2.1 Optimizing quantum Fisher information

A fundamental task in quantum metrology is to attain the ultimate precision limit of estimating some parameter θ , given many copies of a parametrized quantum state $\rho_\theta \in \mathcal{L}(\mathcal{H})$. It is well known that the mean squared error (MSE) $\delta\theta^2$ for an unbiased estimator is bounded, accord-

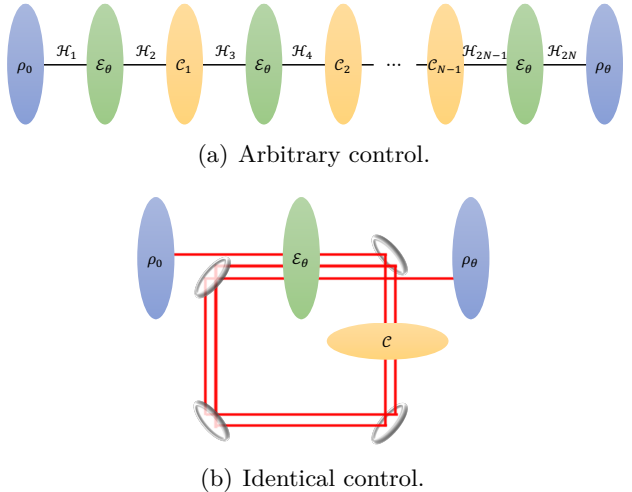


Figure 1: Control-enhanced sequential strategy for estimating θ from N queries to \mathcal{E}_θ , by interleaving $N - 1$ control operations. Each control operation for $i = 1, \dots, N - 1$ is allowed to be an arbitrary quantum channel (CPTP map) \mathcal{C}_i . We can alternatively require all the control operations to be identical $\mathcal{C}_i = \mathcal{C}$, facilitating simpler experimental demonstration as in (b), taking $N = 3$ with two identical control operations for an example. Note that this formalism can be readily generalized to the case with bounded ancilla.

ing to the quantum Cramér-Rao bound (QCRB) [26, 27, 28]

$$\delta\theta^2 \geq \frac{1}{\nu F^Q(\rho_\theta)}, \quad (1)$$

where $F^Q(\rho_\theta)$ is the quantum Fisher information (QFI) and ν is the number of measurements that can be repeated. Importantly, the quantum Cramér-Rao bound is achievable for single-parameter estimation in the limit of $\nu \rightarrow \infty$. Therefore, the QFI is a key figure of merit in quantum metrology, and it is desirable to identify an optimal strategy that is most sensitive to the parameter acquisition and thus yields an output state ρ_θ that maximizes the QFI.

The problem formulation in this work can be illustrated in Fig. 1. Given N queries to a parametrized quantum channel \mathcal{E}_θ , we would like to maximize the QFI of the output state ρ_θ , by preparing an input state ρ_0 and inserting a sequence of control operations $\{\mathcal{C}_i\}_{i=1}^{N-1}$, where each \mathcal{C}_i is a completely positive trace-preserving (CPTP) map. We can also restrict the control operations to be unitary channels $U(\phi_i)$, choosing a variational circuit ansatz for simpler experimental demonstration. Each $\mathcal{E}_\theta \in \mathcal{L}[\mathcal{L}(\mathcal{H}_{2i-1}), \mathcal{L}(\mathcal{H}_{2i})]$, for $i = 1, \dots, N$, and each

$\mathcal{C}_j \in \mathcal{L}[\mathcal{L}(\mathcal{H}_{2j}), \mathcal{L}(\mathcal{H}_{2j+1})]$, for $j = 1, \dots, N - 1$. For simplicity, we assume that the dimension of any \mathcal{H}_i is the same $d = \dim(\mathcal{H}_i)$. We then have the output state

$$\rho_\theta = \Lambda_\theta(\rho_0) = \mathcal{E}_\theta \circ \mathcal{C}_{N-1} \circ \dots \circ \mathcal{C}_2 \circ \mathcal{E}_\theta \circ \mathcal{C}_1 \circ \mathcal{E}_\theta(\rho_0). \quad (2)$$

An optimal strategy is therefore a choice of ρ_0 and $\{\mathcal{C}_i\}$ such that the QFI $F^Q(\rho_\theta)$ is maximal. We assume that no ancilla is used in Fig. 1, but this formulation also applies to the case where an ancilla space of fixed dimension is available, as one can replace \mathcal{E}_θ by $\mathcal{E}_\theta \otimes \mathcal{I}_A$ in the formulation (where A denotes the ancilla space).

By definition, the QFI of a state ρ_θ is given by $F^Q(\rho_\theta) = \text{Tr}(\rho_\theta L_\theta^2)$, where the symmetric logarithmic derivative (SLD) L_θ is the solution to $2\dot{\rho}_\theta = \rho_\theta L_\theta + L_\theta \rho_\theta$, having denoted the derivative of X with respect to θ by \dot{X} . Computing the QFI by this definition, however, is often challenging when the optimization of metrological strategies is concerned. Instead, we can express the QFI $F^Q(\rho_\theta)$ as such a maximization problem [29, 30]:

$$F^Q(\rho_\theta) = \sup_X [2 \text{Tr}(\dot{\rho}_\theta X) - \text{Tr}(\rho_\theta X^2)], \quad (3)$$

where X is a Hermitian operator. One can check that the optimal solution for X is exactly the SLD L_θ . By combining Eq. (2), the maximal QFI obtained from N uses of \mathcal{E}_θ is given by a multivariate maximization:

$$\begin{aligned} F^{(N)}(\mathcal{E}_\theta) &= \sup_{\rho_0, \{\mathcal{C}_i\}} F^Q(\rho_\theta) \\ &= \sup_{\rho_0, \{\mathcal{C}_i\}, X} \left\{ 2 \text{Tr} [\dot{\Lambda}_\theta(\rho_0) X] - \text{Tr} [\Lambda_\theta(\rho_0) X^2] \right\}. \end{aligned} \quad (4)$$

Finding a global maximum for Eq. (4) can be a daunting task. However, considering that $\left\{ 2 \text{Tr} [\dot{\Lambda}_\theta(\rho_0) X] - \text{Tr} [\Lambda_\theta(\rho_0) X^2] \right\}$ is a convex function of each variable in $\{\rho_0, \{\mathcal{C}_i\}, X\}$ while other variables are fixed, in practice we could use an *alternating optimization* method: we search for an optimal solution for each variable by convex optimization, while keeping the other variables fixed, and iteratively repeat the procedure for optimizing all variables in multiple rounds. We remark that similar ideas have also been used for optimizing metrological strategies in many-body systems [6] or with noisy measurements [31]. To implement the optimization in an efficient way for fairly large N , we will introduce the MPO formalism in Section 2.3.

2.2 Choi operator formalism

To facilitate the mapping of the optimization problem Eq. (4) into a tensor network, we first work on the quantum comb formalism [32, 33, 34] and characterize the quantum states and multi-step quantum processes by Choi operators [35] in a unified fashion. The Choi operator of a quantum state ρ is still ρ itself, and the Choi operator of a quantum channel $\mathcal{E} \in \mathcal{L}[\mathcal{L}(\mathcal{H}_{\text{in}}), \mathcal{L}(\mathcal{H}_{\text{out}})]$ is a positive semidefinite operator in $\mathcal{L}(\mathcal{H}_{\text{out}} \otimes \mathcal{H}_{\text{in}})$

$$E = \text{Choi}(\mathcal{E}) := \mathcal{E} \otimes \mathcal{I}(|I\rangle\langle I|), \quad (5)$$

where $|I\rangle\langle I| = \sum_i |i\rangle\langle i|$ is an unnormalized maximally entangled state and $\{|i\rangle\}_i$ is the computational basis of \mathcal{H}_{in} . One can easily check that $\text{Tr}_{\text{out}} E = I_{\text{in}}$. \mathcal{H}_{in} and \mathcal{H}_{out} can take multiple input-output pairs of a certain causal order, corresponding to a multi-step quantum process. The composition of quantum processes \mathcal{A} and \mathcal{B} is then characterized by the link product [33, 34] of Choi operators $A \in \mathcal{L}(\bigotimes_{a \in \mathcal{A}} \mathcal{H}_a)$ and $B \in \mathcal{L}(\bigotimes_{b \in \mathcal{B}} \mathcal{H}_b)$, defined by

$$A * B := \text{Tr}_{\mathcal{A} \cap \mathcal{B}} \left[(I_{\mathcal{B} \setminus \mathcal{A}} \otimes A^{T_{\mathcal{A} \cap \mathcal{B}}}) (B \otimes I_{\mathcal{A} \setminus \mathcal{B}}) \right], \quad (6)$$

where T_i denotes the partial transpose on \mathcal{H}_i , $\mathcal{A} \cap \mathcal{B} := \{i \mid i \in \mathcal{A}, i \in \mathcal{B}\}$, $\mathcal{A} \setminus \mathcal{B} := \{i \mid i \in \mathcal{A}, i \notin \mathcal{B}\}$, and $\mathcal{H}_{\mathcal{X}}$ denotes $\bigotimes_{i \in \mathcal{X}} \mathcal{H}_i$.

With the Choi-Jamiołkowski isomorphism, we denote the Choi operators of $\mathcal{E}_\theta \in \mathcal{L}[\mathcal{L}(\mathcal{H}_{2i-1}), \mathcal{L}(\mathcal{H}_{2i})]$ and $\mathcal{C}_i \in \mathcal{L}[\mathcal{L}(\mathcal{H}_{2i}), \mathcal{L}(\mathcal{H}_{2i+1})]$ by $E_\theta := \text{Choi}(\mathcal{E}_\theta)$ and $C_i := \text{Choi}(\mathcal{C}_i)$. Now we can reformulate Eq. (4) as

$$\begin{aligned} F^{(N)}(\mathcal{E}_\theta) &= \sup_{\rho_0, \{\mathcal{C}_i\}, X} \left\{ 2 \text{Tr} \left[\left(\frac{dE_\theta^{\otimes N}}{d\theta} * \bigotimes_{i=1}^{N-1} C_i \otimes \rho_0 \right) X \right] \right. \\ &\quad \left. - \text{Tr} \left[\left(E_\theta^{\otimes N} * \bigotimes_{i=1}^{N-1} C_i \otimes \rho_0 \right) X^2 \right] \right\}, \end{aligned} \quad (7)$$

where $\rho_0 \geq 0$, $\text{Tr}(\rho_0) = 1$, $C_i \geq 0$, and $\text{Tr}_{2i+1} C_i = I_{2i}$ for any $i = 1, \dots, N - 1$. For ease of notation we define

$$f_1 := \text{Tr} \left[\left(\frac{dE_\theta^{\otimes N}}{d\theta} * \bigotimes_{i=1}^{N-1} C_i \otimes \rho_0 \right) X \right] \quad (8)$$

and

$$f_2 := \text{Tr} \left[\left(E_\theta^{\otimes N} * \bigotimes_{i=1}^{N-1} C_i \otimes \rho_0 \right) X^2 \right]. \quad (9)$$

A main advantage of working with Choi operators is that, it facilitates the optimization of each variable in $\{\rho_0, \{C_i\}, X\}$. While other variables are fixed in the alternating optimization, the optimal solution for each variable in a convex set can be identified either by simple diagonalization or by semidefinite programming (SDP), as we will see later. A naive implementation of the optimization, however, concerns a Hilbert space whose dimension exponentially grows with N . It is essential to compute and optimize $2f_1 - f_2$ efficiently in a tensor network formalism, where all matrices we need to deal with are in the form of MPO.

2.3 Matrix product operators for efficient optimization

MPO is an efficient way to store and manipulate a high-dimensional matrix/tensor. As a simple example, if we would like to store the information of $E_\theta^{\otimes N}$ (where each E_θ is a $d^2 \times d^2$ matrix), we do not need to explicitly store a $d^{2N} \times d^{2N}$ matrix. Instead, it is only necessary to store the information of E_θ , so that we can retrieve each component of $E_\theta^{\otimes N}$ efficiently. To be more specific, we write

$$E_\theta = \sum_{\alpha_{2i}\alpha_{2i-1}\beta_{2i}\beta_{2i-1}} (E_\theta)_{\beta_{2i}\beta_{2i-1}}^{\alpha_{2i}\alpha_{2i-1}} |\alpha_{2i}\alpha_{2i-1}\rangle\langle\beta_{2i}\beta_{2i-1}|, \quad (10)$$

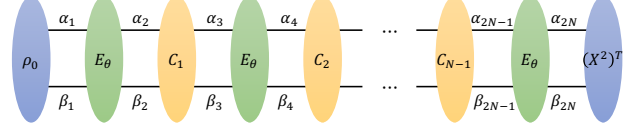
which is an operator in $\mathcal{L}(\mathcal{H}_{2i} \otimes \mathcal{H}_{2i-1})$. We can thus retrieve any component $(E_\theta^{\otimes N})_{\beta_{2N}\dots\beta_{21}}^{\alpha_{2N}\dots\alpha_{21}}$ efficiently with $O(N)$ complexity, by calculating a product $(E_\theta)_{\beta_{2N}\beta_{2N-1}}^{\alpha_{2N}\alpha_{2N-1}} \dots (E_\theta)_{\beta_2\beta_1}^{\alpha_2\alpha_1}$.

The power of MPO is definitely not limited to this simple case of expressing the tensor product of matrices. In fact, MPO ensures the efficiency when the dimension of shared tensor indices (called the bond dimension) can be kept relatively low during tensor contraction. We will see that we can evaluate and optimize f_1 and f_2 (and thus the QFI) in the MPO formalism with a low bond dimension. First, f_2 defined by Eq. (9) is expressed as

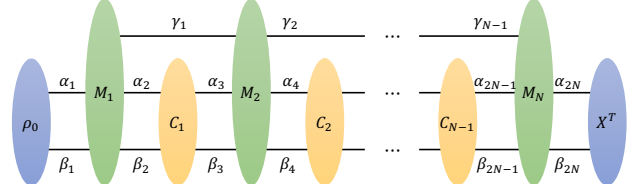
$$f_2 = (X^2)_{\alpha_{2N}}^{\beta_{2N}} (E_\theta)_{\beta_{2N}\beta_{2N-1}}^{\alpha_{2N}\alpha_{2N-1}} \dots (C_1)_{\beta_3\beta_2}^{\alpha_3\alpha_2} (E_\theta)_{\beta_2\beta_1}^{\alpha_2\alpha_1} (\rho_0)_{\beta_1}^{\alpha_1}, \quad (11)$$

having taken the convention of Einstein summation, where repeated indices are implicitly

summed over. This can be schematically illustrated in Fig. 2(a). Each leg represents an index, and a connected line represents a summation over the corresponding index. Computing f_2 requires $O(N)$ complexity.



(a) Tensor network for f_2 .



(b) Tensor network for f_1 .

Figure 2: Tensor networks for computing f_2 in Eq. (9) and f_1 in Eq. (8) for evaluating the QFI. In (b), M_1, \dots, M_N are matrices containing the information about both E_θ and \dot{E}_θ .

Calculating f_1 given by Eq. (8) is a bit more involved, as the derivative $dE_\theta^{\otimes N}/d\theta$ needs to be evaluated. One may simply use $dE_\theta^{\otimes N}/d\theta = \sum_{i=1}^N E_\theta^{\otimes i-1} \otimes \dot{E}_\theta \otimes E_\theta^{\otimes N-i}$, but this introduces an $O(N^2)$ computational overhead, which is unfavorable when N is large. To circumvent this problem, we draw a technique for expressing a sum of local terms as an MPO [36, 37, 38] from many-body Hamiltonian representation. In Appendix A we show that $dE_\theta^{\otimes N}/d\theta$ can be written as an MPO with a bond dimension (corresponding to the γ label) of 2:

$$\frac{dE_\theta^{\otimes N}}{d\theta} = (M_N)_{\beta_{2N}\beta_{2N-1}\gamma_{N-1}}^{\alpha_{2N}\alpha_{2N-1}} \dots (M_2)_{\beta_4\beta_3\gamma_2\gamma_1}^{\alpha_4\alpha_3} (M_1)_{\beta_2\beta_1\gamma_1}^{\alpha_2\alpha_1}, \quad (12)$$

where (for simplicity, we only explicitly focus on the γ indices for the two-dimensional bonds connecting M_1, \dots, M_N)

$$\begin{aligned} (M_N)_1 &= (M_1)_2 = E_\theta, \quad (M_N)_2 = (M_1)_1 = \dot{E}_\theta, \\ (M_i)_{11} &= E_\theta, \quad (M_i)_{12} = \dot{E}_\theta, \\ (M_i)_{21} &= 0, \quad (M_i)_{22} = E_\theta, \\ &\quad \forall i = 2, \dots, N-1. \end{aligned} \quad (13)$$

With the MPO representation of $E_\theta^{\otimes N}/d\theta$, we can easily see that f_1 can be computed as the contraction of a tensor network with $O(N)$ complexity at

a small cost of bond dimension of 2, schematically illustrated in Fig. 2(b). We defer the contraction of f_1 and f_2 in the bounded ancilla case to Appendix B.

The efficiency of a tensor network largely depends on the contraction order of indices. The key idea is to leave open legs as few as possible during the contraction. For our purpose this is simple: we can follow a quantum circuit time flow order (or the reverse order), and the number of open legs would not accumulate. A more detailed complexity analysis of tensor contractions during the optimization will be given in Section 2.4.

2.4 Optimization procedure: arbitrary control

With the tensor networks for f_1 and f_2 , we can now efficiently optimize the QFI $F^{(N)}(\mathcal{E}_\theta) = \sup_{\rho_0, \{C_i\}, X} (2f_1 - f_2)$ by alternating optimization.

We start with an initialization of the input state ρ_0 and the control operations $\{C_i\}$. The initialization can be random, or we can start from a previously known strategy which has a relatively good performance. We can use the tensor network for f_2 without the last tensor $(X^2)^T$ [denoted by $f_2 \setminus (X^2)^T$] to compute the output state ρ_θ , and use the tensor network for f_1 without the last tensor X^T (denoted by $f_1 \setminus X^T$) to compute the derivative $\dot{\rho}_\theta$. We then calculate the SLD of the output state [28]

$$L_\theta = \sum_{jk} \frac{2 \langle j | \dot{\rho}_\theta | k \rangle}{\langle j | \rho_\theta | j \rangle + \langle k | \rho_\theta | k \rangle} |j\rangle\langle k|, \quad (14)$$

where $\rho_\theta = \sum_j \langle j | \rho_\theta | j \rangle |j\rangle\langle j|$ for an orthonormal eigenbasis $\{|j\rangle\}_j$ of ρ_θ . Thus L_θ is the solution for the optimal value of X so far.

Now to update the input state ρ_0 , we contract the tensor network f_1 without the first tensor ρ_0 (denoted by $f_1 \setminus \rho_0$). Similarly, we compute $f_2 \setminus \rho_0$. Our objective is thus to maximize

$$\begin{aligned} (\rho_0)_{\beta_1}^{\alpha_1} (2f_1 \setminus \rho_0 - f_2 \setminus \rho_0)_{\beta_1}^{\alpha_1} \\ = \text{Tr} \left[\rho_0 (2f_1 \setminus \rho_0 - f_2 \setminus \rho_0)^T \right]. \end{aligned} \quad (15)$$

The updated ρ'_0 can be identified as $\rho'_0 = |\psi'_0\rangle\langle\psi'_0|$, where $|\psi'_0\rangle$ is a normalized eigenvector of $(2f_1 \setminus \rho_0 - f_2 \setminus \rho_0)^T$ associated with the maximal eigenvalue. Due to the convexity of QFI, the

optimal input state can always be chosen as a pure state.

For each control operation C_i , we contract $f_1 \setminus C_i$ and $f_2 \setminus C_i$ (with all the tensors updated so far), and compute $2f_1 \setminus C_i - f_2 \setminus C_i$. Without loss of generality, let us take C_1 for example. The optimization of C_1 can be formulated as an SDP:

$$\begin{aligned} \max_{C_1} & \left[(C_1)_{\beta_3 \beta_2}^{\alpha_3 \alpha_2} (2f_1 \setminus C_1 - f_2 \setminus C_1)_{\beta_3 \beta_2}^{\alpha_3 \alpha_2} \right], \\ \text{s.t. } & C_1 \geq 0, \text{Tr}_3 C_1 = I_2. \end{aligned} \quad (16)$$

We can apply similar optimization for C_2, \dots, C_{N-1} . It is important that each C_i is updated by locally solving an optimization problem to circumvent the exponential overhead of a global optimization. Such an optimization procedure is motivated by the well-known algorithm for solving ground states of many-body Hamiltonians via the density matrix renormalization group (DMRG) [39, 40], wherein a matrix product state instead of an MPO representation of control operations is locally and iteratively updated.

It is noteworthy that the constraints in Eq. (16) can be adapted when the control operations are restricted. For instance, if we only allow for entanglement breaking channels [41] as control, then each Choi operator C_i should be optimized over the convex set of (unnormalized) separable states. For the ancilla-free control over a qubit system, the separability of C_i can be fully characterized by the positive partial transpose (PPT) criterion [42, 43], i.e., we require $C_i^{T_{2i}} \geq 0$, where T_{2i} denotes the partial transpose on \mathcal{H}_{2i} . In general for higher-dimensional quantum control operations, the PPT criterion is a necessary but not always sufficient condition for the separability of the Choi operator. In fact, characterizing separability is an NP-hard problem [44]. Nevertheless, the optimization with separability constraints can be approximately solved by a sequence of SDPs with convergence guarantee [45, 46, 47, 48].

We can repeat the procedure above iteratively in an outer loop of optimizing $\{X, \rho_0, \{C_i\}\}$, until the required convergence is satisfied. Finally, we have both the optimized QFI $2f_1 - f_2$ and a concrete strategy to attain it, including a probe state and a set of control operations.

We conclude this section with a complexity analysis of the tensor contraction in each round of the optimization. Assume that \mathcal{E}_θ acts on a d -dimensional system. To update $N + 1$ variable

tensors $\{X, \rho_0, \{C_i\}_{i=1}^{N-1}\}$, we need to contract the tensor network $O(N)$ times. Each contraction of the tensor network for updating a variable requires $O(Nd^4)$ operations by sequentially following a quantum circuit time order or the reverse order. Here the factor d^4 arises from the d^2 values that open indices run over and the d^2 values that connected indices can take, while contracting two tensors each step. In particular, it is important to note that the intermediate results of each contraction can be saved for later use. For example, while updating C_1 , one should keep track of all the intermediate contractions with respect to C_2, \dots, C_{N-1} (in the reverse order). Thus in the next step of updating C_2 , the contraction with respect to C_3, \dots, C_{N-1} can be reused and one only needs to contract the tensor network with the updated C_1 and save the result, which admits $O(d^4)$ computational complexity. Similar arguments hold for updating the remaining tensors. Therefore, each round of the optimization requires $O(Nd^4)$ operations.

2.5 Using identical control operations

In many practical scenarios, for example, for quantum sensors with limited programmability, it is favorable to apply the same control operation at each step. To this end, we propose an alternative approach to optimizing the control operations which are required to be identical, inspired by the infinite MPO (iMPO) [37, 49, 50]. Similar techniques have been used in Ref. [6] for quantum metrology of many-body systems in the infinite particle limit. Note that in this work we employ this technique for finding identical control operations for a finite N .

When the control operations are constrained to be identical, the tensor network optimization becomes a highly nonlinear problem, and we employ a trick to globally update all the control based on the solution from local optimization. First, we need to initialize all the identical control operations $C_i = C$. With a little abuse of the notation, we denote by $2f_1(C) - f_2(C)$ the contraction result of $2f_1 - f_2$ with identical control operations $C_i = C$. In each iteration step, we pick a control operation C_i at random (for example, C_1) and still need to solve an SDP as in Eq. (16), keeping all the tensors fixed except for C_1 . The optimal solution is denoted by \tilde{C}_i . Instead of directly choosing \tilde{C}_i to be the updated control, we

take a convex combination [50]

$$C'_i(\lambda) = \sin^2(\lambda\pi)\tilde{C}_i + \cos^2(\lambda\pi)C_i, \quad (17)$$

for some $\lambda \in [0, 0.5]$ and optimize the choice of λ to maximize $2f_1(C) - f_2(C)$. In practice, it usually works well by performing a local optimization of the variable λ (for example, using the bounded method [51, 52] in SciPy [53]), since we are interested in the convergence result after a number of iterations.

We remark that $2f_1(C) - f_2(C)$ admits fast evaluation even for large N , due to the translation invariant part of the tensor network. Specifically, for evaluating $f_2(C)$, we reshape the tensors as matrices $(\mathbf{E}_\theta)_{\alpha_4\beta_4, \alpha_3\beta_3} = (E_\theta)_{\beta_4\beta_3}^{\alpha_4\alpha_3}$ and $(\mathbf{C})_{\alpha_3\beta_3, \alpha_2\beta_2} = (C)_{\beta_3\beta_2}^{\alpha_3\alpha_2}$. Then instead of contracting a sequence of tensors, we simply compute the power of a matrix

$$\begin{aligned} & [(\mathbf{E}_\theta \mathbf{C})^{N-1}]_{\alpha_{2N}\beta_{2N}, \alpha_2\beta_2} \\ &= (E_\theta)_{\beta_{2N}\beta_{2N-1}}^{\alpha_{2N}\alpha_{2N-1}} C_{\beta_{2N-1}\beta_{2N-2}}^{\alpha_{2N-1}\alpha_{2N-2}} \cdots (E_\theta)_{\beta_4\beta_3}^{\alpha_4\alpha_3} C_{\beta_3\beta_2}^{\alpha_3\alpha_2}, \end{aligned} \quad (18)$$

from which we can easily obtain $f_2(C)$. Analogously, to compute $f_1(C)$, we reshape $(M_i)_{\beta_{2i}\beta_{2i-1}\gamma_i\gamma_{i-1}}^{\alpha_{2i}\alpha_{2i-1}}$ as matrix $\mathbf{M}_{\alpha_{2i}\beta_{2i}\gamma_i, \alpha_{2i-1}\beta_{2i-1}\gamma_{i-1}}$ for $i = 2, \dots, N-1$, and compute the matrix power

$$\begin{aligned} & \{[\mathbf{M}(\mathbf{C} \otimes I)]^{N-2}\}_{\alpha_{2N-2}\beta_{2N-2}\gamma_{N-1}, \alpha_2\beta_2} \\ &= (M_{N-1})_{\beta_{2N-2}\beta_{2N-3}\gamma_{N-1}\gamma_{N-2}}^{\alpha_{2N-2}\alpha_{2N-3}} C_{\beta_{2N-3}\beta_{2N-4}}^{\alpha_{2N-3}\alpha_{2N-4}} \cdots \\ & \quad (M_2)_{\beta_4\beta_3\gamma_2\gamma_1}^{\alpha_4\alpha_3} C_{\beta_3\beta_2}^{\alpha_3\alpha_2}, \end{aligned} \quad (19)$$

from which $f_1(C)$ can be immediately obtained.

2.6 Variational unitary control

Implementing an arbitrary CPTP control operation is sometimes challenging. To be more experiment-friendly, we can alternatively take a simple variational ansatz for the control (see Appendix C), and thus characterize each control by several variational parameters. In this case $C_i = \text{Choi}[\mathcal{U}(\phi_i)]$ is the Choi operator of the variational circuit unitary $U(\phi_i)$, where ϕ_i is a vector of variational parameters for the i -th control operation, and $\mathcal{U}(\phi_i)(\rho) = U(\phi_i)\rho[U(\phi_i)]^\dagger$.

Previously variational circuits have been mostly used for optimizing small-scale problems in quantum metrology [54, 55, 56, 57, 58, 59, 18].

The tensor network formulation here, however, allows for optimizing a long sequence of variational control operations efficiently. Concatenating the variational ansatz with the tensor network algorithm, we employ a local update method if each control operation can be different, and a global update method if all the control operations are restricted to be identical.

2.6.1 Local update: arbitrary variational parameters

We first introduce the local update method, which is just a slight modification of the optimization procedure introduced in Section 2.4. Instead of solving an SDP for each control operation C_i , each time we fix X , ρ_0 , and all the other control $\{U(\phi_j)\}_{j \neq i}$, take the cost function $-[2f_1(\phi_i) - f_2(\phi_i)]$ as a function of ϕ_i , and tune the variational parameters ϕ_i by gradient descent to minimize the cost function. The gradient estimation is both time-efficient and memory-efficient as each variational control is locally updated.

2.6.2 Global update: identical variational parameters

For a simpler experimental demonstration of quantum sensors, we can further restrict $\phi_i = \phi$ for all control operations, admitting a succinct circuit description. To update the variational parameters ϕ in each iteration, we need to estimate the gradient with respect to ϕ :

$$\begin{aligned} & \nabla_\phi (f_2 - 2f_1) \\ &= \nabla_\phi C_{\beta_3 \beta_2}^{\alpha_3 \alpha_2} \sum_i (f_2 \langle C_i - 2f_1 \rangle C_i)_{\beta_3 \beta_2}^{\alpha_3 \alpha_2}, \end{aligned} \quad (20)$$

where $C_i = C = \text{Choi}[\mathcal{U}(\phi)]$ for all $i = 1, \dots, N-1$. Note that we can efficiently compute the summation over the control index i by sharing intermediate contraction results in a similar fashion as in Section 2.4.

3 Numerical experiments

In this section, we apply the algorithms introduced above to different noise models for $N = 2$ to $N = 100$ queries. For the first example, phase estimation with the bit flip noise can achieve the Heisenberg limit (HL) $[F^{(N)}(\mathcal{E}_\theta) \propto N^2]$. When N

is finite, our algorithm can outperform the state-of-the-art asymptotically optimal approach based on QEC [16, 17, 14] as well as other known strategies. For the second example of the amplitude damping noise, it is known a priori that the standard quantum limit (SQL) $[F^{(N)}(\mathcal{E}_\theta) \propto N]$ can be attained with unbounded ancilla [14], but when the ancilla is bounded a theoretical analysis of the optimal metrological performance is lacking. Here, our algorithm can yield control strategies that significantly outperform a control-free one. Note that in this work we take the convention that signal comes after noise as in Ref. [15], which is more interesting in some scenarios, where the HL can be achieved in noisy channel estimation, but the coefficient of the scaling is smaller than the noiseless case. As a final example of non-unitary encoding, we investigate the estimation of the direction angle of the dephasing noise by our algorithm.

To achieve faster convergence¹, we may try starting from a known strategy (e.g., QEC), or initialize the configuration in an adaptive way: we choose the input state and control operations based on the optimized strategy for N queries, as a starting point for optimizing the strategy with $N+1$ queries. The algorithm typically converges well in around 50–200 iterations.

3.1 Phase estimation with the bit flip noise

We start with the extensively studied bit flip noise model, and compare our results with some existing works. In the ancilla-free scenario, our result matches a recent finding [64] for achieving the SQL. Assisted by one ancilla, our result outperforms the asymptotically optimal QEC strategy [16, 17, 14] by using CPTP control, and outperforms the best known ancilla-free strategy by using unitary control. A summary of known results of the asymptotic QFI for comparison is given in Table 1.

¹In some cases it may also be helpful to add some perturbation (for example, an additional depolarizing noise decaying versus iterations) to the channel to estimate \mathcal{E}_θ . We suspect that this may help circumvent the possible discontinuity of the QFI at the parameter value where the rank of the output state ρ_θ changes [60, 61, 62, 63].

Table 1: Known scalings of the QFI for phase estimation with the bit flip noise by control-enhanced sequential strategies.

Control type	CPTP	Unitary
No ancilla [64]	$O(N^{1.5})$	$\Theta(N)$
Bounded ancilla	$\Theta(N^2)$ [65]	$\Theta(N)$ [64]
Unbounded ancilla [65]	$\Theta(N^2)$	$\Theta(N^2)$

We would like to estimate θ from N queries to a quantum channel \mathcal{E}_θ described by the Kraus operators $\{K_i^\theta = U_Z(\theta)K_i^{(\text{BF})}\}_{i=1}^2$, where $U_Z(\theta) = e^{-i\theta\sigma_z/2}$ and

$$K_1^{(\text{BF})} = \sqrt{1-p}I, \quad K_2^{(\text{BF})} = \sqrt{p}\sigma_x, \quad (21)$$

for $0 \leq p \leq 1$. In numerical experiments, we take $p = 0.1$ and the ground truth $\theta = \theta_0 = 1.0$.

We compare the normalized QFI $F^{(N)}(\mathcal{E}_\theta)/N$ obtained by different strategies versus N for $N = 2$ to 100 queries to \mathcal{E}_θ in Fig. 3. First, in the ancilla-free scenario, we apply the optimization algorithms using arbitrary/identical, CPTP/variational unitary control operations. In all these 4 cases the obtained results coincide with each other: the growth of $F^{(N)}(\mathcal{E}_\theta)/N$ slows down as N increases, which implies a standard quantum scaling. We further find out that the control operation U_c output by our algorithm is very close to the inverse of the unitary encoding the signal at the ground truth $\theta = \theta_0$:

$$U_c \approx U_Z(\theta_0)^\dagger. \quad (22)$$

This result matches the theoretical finding in a recent work [64, Theorem 5], which states that for this noise model the SQL can be achieved in the asymptotic limit by nearly reversing the signal encoding unitary, such that $\lim_{N \rightarrow \infty} F^{(N)}(\mathcal{E}_\theta)/N$ can be arbitrarily close to $\frac{1-p}{p}$ [64], depicted as a dashed gray line in Fig. 3 for comparison².

Next, we investigate the performance of the strategy assisted by one ancilla qubit. In this case, an asymptotically optimal QEC strategy requiring one ancilla is known [14] and yields the HL $\lim_{N \rightarrow \infty} F^{(N)}(\mathcal{E}_\theta)/N^2 = (1-2p)^2$. However, the QEC is not optimal for a finite N [15, 18, 19].

²It is worth noting that, however, exactly choosing $U_c = U_Z(\theta_0)^\dagger$ results in the discontinuity of the QFI, as the matrix rank of the output state ρ_θ changes at this point of $\theta = \theta_0$, and this can also cause the numerical instability of the algorithm.

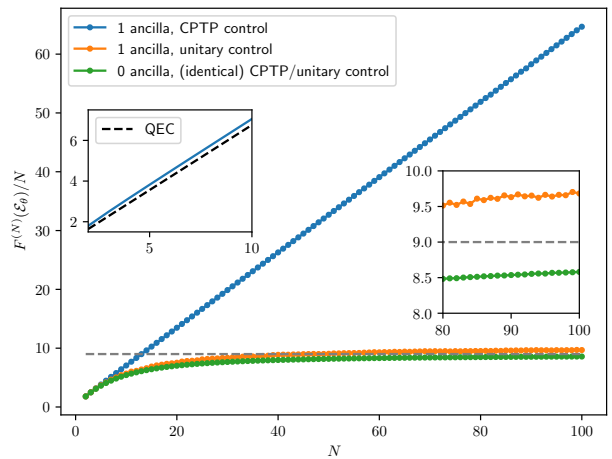


Figure 3: The normalized QFI $F^{(N)}(\mathcal{E}_\theta)/N$ versus the number of queries N to \mathcal{E}_θ for phase estimation with the bit flip noise. The left inset figure shows that $F^{(N)}(\mathcal{E}_\theta)/N$ assisted by 1 ancilla and CPTP control operations (solid blue line) can be higher than that obtained by an optimal QEC strategy (dashed black line) for $N = 2$ to 10. This advantage will become smaller when N is larger (but still exists for $N = 100$), which is expected as the QEC strategy is asymptotically optimal. The right inset shows that, with 1 ancilla and unitary control (solid orange line), $F^{(N)}(\mathcal{E}_\theta)/N$ can surpass the asymptotic limit of the ancilla-free strategy (dashed gray line) proposed in Ref. [64] when N is large enough.

Fig. 3 shows that the QFI yielded by using arbitrary CPTP control can outperform that yielded by an optimal QEC strategy. To make a fair comparison, we apply $N-1$ QEC recovery operations between \mathcal{E}_θ and exclude the final recovery operation (which maps the state back to the codespace) at the end. We also make sure that QEC approximately reverses the effect of the signal unitary (up to a unitary $e^{-i\epsilon\sigma_z/2}$ with a small $\epsilon = 0.01$), otherwise the QFI obtained from QEC may significantly decrease due to the discontinuity. We illustrate the metrological performance gap between the QEC strategy and the tensor network algorithm for $N = 2$ to 10 in the left inset of Fig. 3. When N gets large (e.g., $N \approx 100$), the relative advantage becomes smaller but still exists. We expect that the relative gap would vanish in the asymptotic limit, as the QEC strategy is asymptotically optimal. Nevertheless, our algorithm provides a higher metrological sensitivity in real-world experiments with finite N .

Moreover, by using variational unitary control operations with one ancilla qubit, our algorithm yields a normalized QFI $F^{(N)}(\mathcal{E}_\theta)/N$ higher

than the theoretical limit $\frac{1-p}{p}$ of the best existing ancilla-free strategy [64], depicted by the right inset of Fig. 3 for $N = 80$ to 100. Our results indicate that, even if the QFI with unitary control and bounded ancilla can only achieve the SQL [64] as in the ancilla-free case, the ancilla could still be useful by improving the coefficient of the scaling.

3.2 Phase estimation with the amplitude damping noise

With the amplitude damping noise, the channel to estimate \mathcal{E}_θ is characterized by the Kraus operators $\{K_i^\theta = U_Z(\theta)K_i^{(\text{AD})}\}_{i=1}^2$, where

$$K_1^{(\text{AD})} = \begin{pmatrix} 1 & 0 \\ 0 & \sqrt{1-p} \end{pmatrix}, \quad K_2^{(\text{AD})} = \begin{pmatrix} 0 & \sqrt{p} \\ 0 & 0 \end{pmatrix}, \quad (23)$$

for $0 \leq p \leq 1$. In contrast to the previous example (i.e., the bit flip model), under amplitude damping noise, phase estimation cannot achieve the HL even with unbounded ancilla [9, 10, 11]. A summary of known scalings of QFI is presented in Table 2.

Table 2: Known scalings of the QFI for phase estimation with the amplitude damping noise by control-enhanced sequential strategies.

Control type	CPTP	Unitary
No ancilla [64]	$\Theta(1)$	$O(1)$
Bounded ancilla [13]	$O(N)$	$O(N)$
Unbounded ancilla [13, 14]	$\Theta(N)$	$\Theta(N)$

Unlike the bit flip noise model, for the amplitude damping noise it was only known that attaining the SQL requires an unbounded memory cost linear in N [14]. Here with bounded ancilla, we identified several strategies yielding QFI following the linear trend for large N .

We take $p = 0.1$ and the true value of the parameter $\theta_0 = 1.0$, and optimize the QFI $F^{(N)}(\mathcal{E}_\theta)$ with different strategies, as illustrated in Fig. 4. Since there is no known strategy with bounded ancilla for this noise model, we use as a benchmark the QFI obtained by a control-free strategy with the input state $|+\rangle = \frac{1}{\sqrt{2}}(|0\rangle + |1\rangle)$, represented as a dashed line. In the ancilla-free case, we note that using different control operations can provide a slight enhancement compared to

identical control operations, but we find no performance gaps between CPTP and unitary control. Assisted by one ancilla qubit, using CPTP control yields a QFI $F^{(N)}(\mathcal{E}_\theta)$ nearly linear in N when N is large. It may be interesting to theoretically investigate whether the SQL is achievable with one ancilla, which is an open problem so far. Moreover, unitary control in the ancilla-assisted case can significantly outperform generic CPTP control in the ancilla-free case. We also remark that all the 4 control strategies have different performances in the ancilla-assisted case.

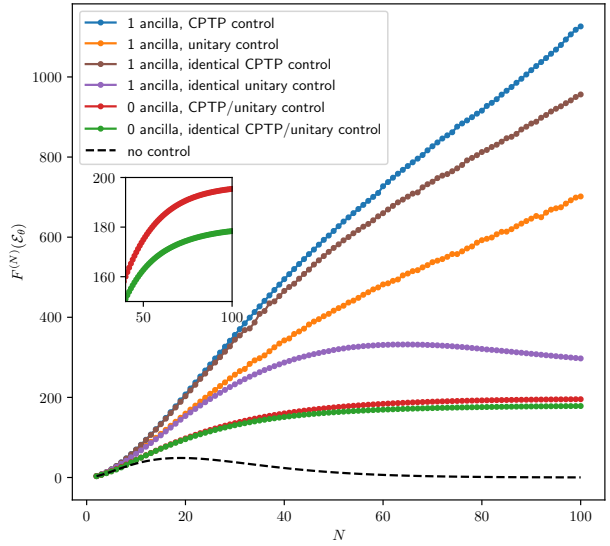


Figure 4: The QFI $F^{(N)}(\mathcal{E}_\theta)$ versus the number of queries N to \mathcal{E}_θ for phase estimation with the amplitude damping noise. We zoom in on the interval $[40, 100]$ of N to more clearly demonstrate the advantage of using different control over identical control with ancilla-free strategies. As a benchmark, the dashed black line is obtained by an ancilla-free and control-free strategy with the input state $|+\rangle = \frac{1}{\sqrt{2}}(|0\rangle + |1\rangle)$.

3.3 Dephasing direction estimation

In preceding examples we have applied our approach to phase estimation in the presence of noise. Here we consider a problem of non-unitary encoding, where we would like to estimate the dephasing direction angle θ from N queries to \mathcal{E}_θ characterized by the Kraus operators

$$K_1^{\theta,(\text{dep})} = \sqrt{1-p}I, \\ K_2^{\theta,(\text{dep})} = \sqrt{p}(\cos\theta\sigma_z + \sin\theta\sigma_x), \quad (24)$$

for $0 \leq p \leq 1$. Known scalings of QFI for this model is the same as the scalings presented in

Table 1, implying that the HL is attainable by QEC.

We take $p = 0.1$ and the ground truth $\theta_0 = 1.0$, and apply our algorithm to optimize the QFI $F^{(N)}(\mathcal{E}_\theta)$ with restricted ancilla and control. Specifically, here we focus on the QFI attainable by identical unitary control with zero or one ancilla qubit, as more complicated control strategies do not offer large advantages. The results of QFI versus N are plotted in Fig. 5. Clearly, there is an advantage of employing coherence, as using identical unitary control can outperform a classical strategy where N channels are estimated independently, and using ancilla is indeed advantageous.

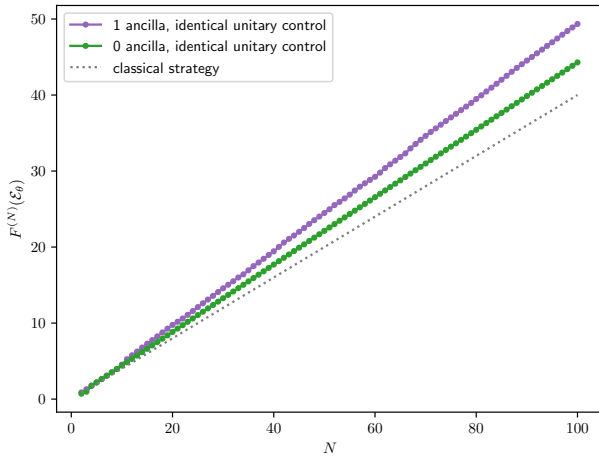


Figure 5: The QFI $F^{(N)}(\mathcal{E}_\theta)$ versus the number of queries N to \mathcal{E}_θ for dephasing direction angle estimation. The classical strategy (dotted gray line) independently estimates N channels, yielding a total QFI as the N -fold single channel QFI $NF^{(1)}(\mathcal{E}_\theta)$.

4 Discussion

We have provided an efficient approach to optimizing control-enhanced metrological strategies by leveraging tensor networks. With its high flexibility for applying arbitrary or identical control operations and assigning the ancilla dimension, we anticipate that this approach is well-suited for real-world experimental demonstration under certain restrictions. This may be particularly suitable for optical experiments, where typically the same control is applied each time with no or small ancilla in an optical loop [20, 21].

Our approach naturally extends its applicability beyond single-parameter quantum chan-

nel estimation. An immediate application is in Hamiltonian parameter estimation with Markovian noise [16, 17, 66], where our framework can be used to identify how the frequency of fast quantum control affects the metrological performance. We can also relax the assumption of estimating N independent channels, but investigate the case where the non-Markovian noise takes effect, induced by the environment which has memory effect [67, 68, 18]. In this case the non-Markovian process can still be expressed as an MPO, with the bond dimension corresponding to the memory [69, 70, 71], so our formalism can also be applicable. Besides, it could be interesting to generalize our framework to multi-parameter Hamiltonian estimation, where the asymptotically optimal QEC protocol has been identified by SDP previously [72]. Finally, an exciting future work could be developing an efficient approach, possibly based on tensor networks combining the techniques of Ref. [6] and our work, to optimizing quantum metrology for many-body systems with multi-step control, which handles both spatial complexity and temporal complexity in a unified framework.

Acknowledgements

This work is supported by the National Natural Science Foundation of China via Excellent Young Scientists Fund (Hong Kong and Macau) Project 12322516, Guangdong Basic and Applied Basic Research Foundation (Project No. 2022A1515010340), Guangdong Provincial Quantum Science Strategic Initiative (No. GDZX2303007), and the Hong Kong Research Grant Council (RGC) through the Early Career Scheme (ECS) grant 27310822 and the General Research Fund (GRF) grant 17303923. The numerical results are obtained via the Python packages `opt_einsum` [73], `CVXPY` [74, 75] with the solver `MOSEK` [76], and `PennyLane` [77]. The code accompanying the paper is available on GitHub [78].

Note added.—After the completion of this work, we learned about an independent work using similar approaches [79].

References

- [1] Vittorio Giovannetti, Seth Lloyd, and Lorenzo Maccone. “Quantum-enhanced measurements: Beating the standard quantum limit”. *Science* **306**, 1330–1336 (2004).
- [2] Vittorio Giovannetti, Seth Lloyd, and Lorenzo Maccone. “Quantum Metrology”. *Phys. Rev. Lett.* **96**, 010401 (2006).
- [3] C. L. Degen, F. Reinhard, and P. Cappellaro. “Quantum sensing”. *Rev. Mod. Phys.* **89**, 035002 (2017).
- [4] Hsin-Yuan Huang, Yu Tong, Di Fang, and Yuan Su. “Learning many-body hamiltonians with heisenberg-limited scaling”. *Phys. Rev. Lett.* **130**, 200403 (2023).
- [5] Yaoming Chu, Xiangbei Li, and Jianming Cai. “Strong quantum metrological limit from many-body physics”. *Phys. Rev. Lett.* **130**, 170801 (2023).
- [6] Krzysztof Chabuda, Jacek Dziarmaga, Tobias J. Osborne, and Rafał Demkowicz-Dobrzański. “Tensor-network approach for quantum metrology in many-body quantum systems”. *Nat. Commun.* **11**, 250 (2020).
- [7] Chao Yin and Andrew Lucas. “Heisenberg-limited metrology with perturbing interactions”. *Quantum* **8**, 1303 (2024).
- [8] Alicja Dutkiewicz, Thomas E. O’Brien, and Thomas Schuster. “The advantage of quantum control in many-body Hamiltonian learning”. *Quantum* **8**, 1537 (2024).
- [9] Akio Fujiwara and Hiroshi Imai. “A fibre bundle over manifolds of quantum channels and its application to quantum statistics”. *J. Phys. A* **41**, 255304 (2008).
- [10] B. M. Escher, R. L. de Matos Filho, and L. Davidovich. “General framework for estimating the ultimate precision limit in noisy quantum-enhanced metrology”. *Nat. Phys.* **7**, 406–411 (2011).
- [11] Rafał Demkowicz-Dobrzański, Jan Kołodyński, and Mădălin Guță. “The elusive heisenberg limit in quantum-enhanced metrology”. *Nat. Commun.* **3**, 1063 (2012).
- [12] Jan Kołodyński and Rafał Demkowicz-Dobrzański. “Efficient tools for quantum metrology with uncorrelated noise”. *New J. Phys.* **15**, 073043 (2013).
- [13] Rafal Demkowicz-Dobrzański and Lorenzo Maccone. “Using entanglement against noise in quantum metrology”. *Phys. Rev. Lett.* **113**, 250801 (2014).
- [14] Sisi Zhou and Liang Jiang. “Asymptotic theory of quantum channel estimation”. *PRX Quantum* **2**, 010343 (2021).
- [15] Stanisław Kurdziałek, Wojciech Górecki, Francesco Albarelli, and Rafał Demkowicz-Dobrzański. “Using adaptiveness and causal superpositions against noise in quantum metrology”. *Phys. Rev. Lett.* **131**, 090801 (2023).
- [16] Rafał Demkowicz-Dobrzański, Jan Czajkowski, and Pavel Sekatski. “Adaptive Quantum Metrology under General Markovian Noise”. *Phys. Rev. X* **7**, 041009 (2017).
- [17] Sisi Zhou, Mengzhen Zhang, John Preskill, and Liang Jiang. “Achieving the heisenberg limit in quantum metrology using quantum error correction”. *Nat. Commun.* **9**, 78 (2018).
- [18] Anian Altherr and Yuxiang Yang. “Quantum metrology for non-markovian processes”. *Phys. Rev. Lett.* **127**, 060501 (2021).
- [19] Qiushi Liu, Zihao Hu, Haidong Yuan, and Yuxiang Yang. “Optimal strategies of quantum metrology with a strict hierarchy”. *Phys. Rev. Lett.* **130**, 070803 (2023).
- [20] Zhibo Hou, Rui-Jia Wang, Jun-Feng Tang, Haidong Yuan, Guo-Yong Xiang, Chuan-Feng Li, and Guang-Can Guo. “Control-Enhanced Sequential Scheme for General Quantum Parameter Estimation at the Heisenberg Limit”. *Phys. Rev. Lett.* **123**, 040501 (2019).
- [21] Zhibo Hou, Yan Jin, Hongzhen Chen, Jun-Feng Tang, Chang-Jiang Huang, Haidong Yuan, Guo-Yong Xiang, Chuan-Feng Li, and Guang-Can Guo. ““super-heisenberg” and heisenberg scalings achieved simultaneously in the estimation of a rotating field”. *Phys. Rev. Lett.* **126**, 070503 (2021).
- [22] Román Orús. “A practical introduction to tensor networks: Matrix product states and projected entangled pair states”. *Ann. Phys. (N. Y.)* **349**, 117–158 (2014).

[23] Jacob C Bridgeman and Christopher T Chubb. “Hand-waving and interpretive dance: an introductory course on tensor networks”. *J. Phys. A* **50**, 223001 (2017).

[24] Giacomo Torlai, Christopher J. Wood, Atithi Acharya, Giuseppe Carleo, Juan Carrasquilla, and Leandro Aolita. “Quantum process tomography with unsupervised learning and tensor networks”. *Nat. Commun.* **14**, 2858 (2023).

[25] Chu Guo, Kavan Modi, and Dario Poletti. “Tensor-network-based machine learning of non-markovian quantum processes”. *Phys. Rev. A* **102**, 062414 (2020).

[26] Carl W. Helstrom. “Quantum detection and estimation theory”. Academic Press. New York (1976).

[27] Alexander S. Holevo. “Probabilistic and statistical aspects of quantum theory”. North-Holland Publishing Company. Amsterdam (1982).

[28] Samuel L. Braunstein and Carlton M. Caves. “Statistical distance and the geometry of quantum states”. *Phys. Rev. Lett.* **72**, 3439–3443 (1994).

[29] Katarzyna Macieszczak. “Quantum fisher information: Variational principle and simple iterative algorithm for its efficient computation” (2013). [arXiv:1312.1356](https://arxiv.org/abs/1312.1356).

[30] Katarzyna Macieszczak, Martin Fraas, and Rafał Demkowicz-Dobrzański. “Bayesian quantum frequency estimation in presence of collective dephasing”. *New J. Phys.* **16**, 113002 (2014).

[31] Yink Loong Len, Tuvia Gefen, Alex Retzker, and Jan Kołodyński. “Quantum metrology with imperfect measurements”. *Nat. Commun.* **13**, 6971 (2022).

[32] Gus Gutoski and John Watrous. “Toward a general theory of quantum games”. In *Proceedings of the Thirty-Ninth Annual ACM Symposium on Theory of Computing*. Page 565–574. New York, NY, USA (2007). Association for Computing Machinery.

[33] G. Chiribella, G. M. D’Ariano, and P. Perinotti. “Quantum Circuit Architecture”. *Phys. Rev. Lett.* **101**, 060401 (2008).

[34] Giulio Chiribella, Giacomo Mauro D’Ariano, and Paolo Perinotti. “Theoretical framework for quantum networks”. *Phys. Rev. A* **80**, 022339 (2009).

[35] Man-Duen Choi. “Completely positive linear maps on complex matrices”. *Linear Algebra Appl.* **10**, 285–290 (1975).

[36] Gregory M. Crosswhite and Dave Bacon. “Finite automata for caching in matrix product algorithms”. *Phys. Rev. A* **78**, 012356 (2008).

[37] I. P. McCulloch. “Infinite size density matrix renormalization group, revisited” (2008). [arXiv:0804.2509](https://arxiv.org/abs/0804.2509).

[38] C. Hubig, I. P. McCulloch, and U. Schollwöck. “Generic construction of efficient matrix product operators”. *Phys. Rev. B* **95**, 035129 (2017).

[39] Steven R. White. “Density matrix formulation for quantum renormalization groups”. *Phys. Rev. Lett.* **69**, 2863–2866 (1992).

[40] Steven R. White. “Density-matrix algorithms for quantum renormalization groups”. *Phys. Rev. B* **48**, 10345–10356 (1993).

[41] Michael Horodecki, Peter W. Shor, and Mary Beth Ruskai. “Entanglement breaking channels”. *Rev. Math. Phys.* **15**, 629–641 (2003).

[42] Asher Peres. “Separability criterion for density matrices”. *Phys. Rev. Lett.* **77**, 1413–1415 (1996).

[43] Michał Horodecki, Paweł Horodecki, and Ryszard Horodecki. “Separability of mixed states: necessary and sufficient conditions”. *Phys. Lett. A* **223**, 1–8 (1996).

[44] Leonid Gurvits. “Classical deterministic complexity of edmonds’ problem and quantum entanglement”. In *Proceedings of the Thirty-Fifth Annual ACM Symposium on Theory of Computing*. Page 10–19. New York, NY, USA (2003). Association for Computing Machinery.

[45] A. C. Doherty, Pablo A. Parrilo, and Federico M. Spedalieri. “Distinguishing separable and entangled states”. *Phys. Rev. Lett.* **88**, 187904 (2002).

[46] Andrew C. Doherty, Pablo A. Parrilo, and Federico M. Spedalieri. “Complete family

of separability criteria”. *Phys. Rev. A* **69**, 022308 (2004).

[47] Xiao-Dong Yu, Timo Simnacher, Nikolai Wyderka, H. Chau Nguyen, and Otfried Ghne. “A complete hierarchy for the pure state marginal problem in quantum mechanics”. *Nat. Commun.* **12**, 1012 (2021).

[48] Xiao-Dong Yu, Timo Simnacher, H. Chau Nguyen, and Otfried Ghne. “Quantum-inspired hierarchy for rank-constrained optimization”. *PRX Quantum* **3**, 010340 (2022).

[49] L. Cincio and G. Vidal. “Characterizing topological order by studying the ground states on an infinite cylinder”. *Phys. Rev. Lett.* **110**, 067208 (2013).

[50] Philippe Corboz. “Variational optimization with infinite projected entangled-pair states”. *Phys. Rev. B* **94**, 035133 (2016).

[51] George E. Forsythe, Michael A. Malcolm, and Cleve B. Moler. “Computer methods for mathematical computations”. Prentice Hall Professional Technical Reference. (1977).

[52] Richard P. Brent. “Algorithms for minimization without derivatives”. Courier Corporation. (2013).

[53] Pauli Virtanen *et al.* “SciPy 1.0: Fundamental Algorithms for Scientific Computing in Python”. *Nat. Methods* **17**, 261–272 (2020).

[54] Blnt Koczor, Suguru Endo, Tyson Jones, Yuichiro Matsuzaki, and Simon C Benjamin. “Variational-state quantum metrology”. *New J. Phys.* **22**, 083038 (2020).

[55] Xiaodong Yang, Jayne Thompson, Ze Wu, Mile Gu, Xinhua Peng, and Jiangfeng Du. “Probe optimization for quantum metrology via closed-loop learning control”. *npj Quantum Inf.* **6**, 62 (2020).

[56] Ziqi Ma, Pranav Gokhale, Tian-Xing Zheng, Sisi Zhou, Xiaofei Yu, Liang Jiang, Peter Maurer, and Frederic T. Chong. “Adaptive circuit learning for quantum metrology”. In 2021 IEEE International Conference on Quantum Computing and Engineering (QCE). Pages 419–430. (2021).

[57] Johannes Jakob Meyer, Johannes Borregaard, and Jens Eisert. “A variational toolbox for quantum multi-parameter estimation”. *npj Quantum Inf.* **7**, 89 (2021).

[58] Jacob L. Beckey, M. Cerezo, Akira Sone, and Patrick J. Coles. “Variational quantum algorithm for estimating the quantum fisher information”. *Phys. Rev. Res.* **4**, 013083 (2022).

[59] Trung Kien Le, Hung Q. Nguyen, and Le Bin Ho. “Variational quantum metrology for multiparameter estimation under dephasing noise”. *Sci. Rep.* **13**, 17775 (2023).

[60] Dominik afrnek. “Discontinuities of the quantum fisher information and the bures metric”. *Phys. Rev. A* **95**, 052320 (2017).

[61] Luigi Seveso, Francesco Albarelli, Marco G Genoni, and Matteo G A Paris. “On the discontinuity of the quantum fisher information for quantum statistical models with parameter dependent rank”. *J. Phys. A* **53**, 02LT01 (2019).

[62] Sisi Zhou and Liang Jiang. “An exact correspondence between the quantum fisher information and the bures metric” (2019). [arXiv:1910.08473](https://arxiv.org/abs/1910.08473).

[63] Yating Ye and Xiao-Ming Lu. “Quantum cramr-rao bound for quantum statistical models with parameter-dependent rank”. *Phys. Rev. A* **106**, 022429 (2022).

[64] Sisi Zhou. “Limits of noisy quantum metrology with restricted quantum controls”. *Phys. Rev. Lett.* **133**, 170801 (2024).

[65] E. M. Kessler, I. Lovchinsky, A. O. Sushkov, and M. D. Lukin. “Quantum error correction for metrology”. *Phys. Rev. Lett.* **112**, 150802 (2014).

[66] Pavel Sekatski, Michalis Skotiniotis, Janek Kodyski, and Wolfgang Dr. “Quantum metrology with full and fast quantum control”. *Quantum* **1**, 27 (2017).

[67] Alex W. Chin, Susana F. Huelga, and Martin B. Plenio. “Quantum metrology in non-markovian environments”. *Phys. Rev. Lett.* **109**, 233601 (2012).

[68] Yuxiang Yang. “Memory effects in quantum metrology”. *Phys. Rev. Lett.* **123**, 110501 (2019).

[69] Felix A. Pollock, Csar Rodrguez-Rosario, Thomas Frauenheim, Mauro Paternostro,

and Kavan Modi. “Non-markovian quantum processes: Complete framework and efficient characterization”. *Phys. Rev. A* **97**, 012127 (2018).

[70] Felix A. Pollock, César Rodríguez-Rosario, Thomas Frauenheim, Mauro Paternostro, and Kavan Modi. “Operational markov condition for quantum processes”. *Phys. Rev. Lett.* **120**, 040405 (2018).

[71] Eoin P. Butler, Gerald E. Fux, Carlos Ortega-Taberner, Brendon W. Lovett, Jonathan Keeling, and Paul R. Eastham. “Optimizing performance of quantum operations with non-markovian decoherence: The tortoise or the hare?”. *Phys. Rev. Lett.* **132**, 060401 (2024).

[72] Wojciech Górecki, Sisi Zhou, Liang Jiang, and Rafał Demkowicz-Dobrzański. “Optimal probes and error-correction schemes in multi-parameter quantum metrology”. *Quantum* **4**, 288 (2020).

[73] Daniel G. a. Smith and Johnnie Gray. “opt_einsum - a python package for optimizing contraction order for einsum-like expressions”. *J. Open Source Softw.* **3**, 753 (2018).

[74] Steven Diamond and Stephen Boyd. “Cvxpy: a python-embedded modeling language for convex optimization”. *J. Mach. Learn. Res.* **17**, 2909–2913 (2016). url: <https://dl.acm.org/doi/10.5555/2946645.3007036>.

[75] Steven Diamond, Akshay Agrawal, Robin Verschueren and Stephen Boyd. “A rewriting system for convex optimization problems”. *J. Control Decis.* **5**, 42–60 (2018).

[76] MOSEK ApS. “The mosek optimizer api for python manual. version 9.3.”. (2021). url: <https://docs.mosek.com/9.3/pythonapi/index.html>.

[77] Ville Bergholm *et al.* “Pennylane: Automatic differentiation of hybrid quantum-classical computations” (2022). [arXiv:1811.04968](https://arxiv.org/abs/1811.04968).

[78] Qiushi Liu and Yuxiang Yang. “Tensor network algorithm for optimizing control-enhanced quantum metrology”. https://github.com/qiushi-liu/tensor_network_metrology (2024).

[79] Stanislaw Kurdzialek, Piotr Dulian, Joanna Majsak, Sagnik Chakraborty, and Rafal Demkowicz-Dobrzanski. “Quantum metrology using quantum combs and tensor network formalism” (2024). [arXiv:2403.04854](https://arxiv.org/abs/2403.04854).

[80] Michael A. Nielsen and Isaac L. Chuang. “Quantum computation and quantum information: 10th anniversary edition”. Cambridge University Press. Cambridge (2010).

[81] John Duchi, Elad Hazan, and Yoram Singer. “Adaptive subgradient methods for online learning and stochastic optimization”. *J. Mach. Learn. Res.* **12**, 2121–2159 (2011). url: <https://dl.acm.org/doi/10.5555/1953048.2021068>.

A Proof of Eq. (12)

It is not difficult to verify that Eq. (12) is equivalent to $dE_\theta^{\otimes N}/d\theta = \sum_{i=1}^N E_\theta^{\otimes i-1} \otimes \dot{E}_\theta \otimes E_\theta^{\otimes N-i}$. Nevertheless, here we provide a diagrammatic method [36] to derive this result in an intuitive way, which has been widely used in compressing sum of local Hamiltonian terms into an MPO.

Without loss of generality, let us consider the case of $N = 4$. Then $dE_\theta^{\otimes 4}/d\theta = \sum_{i=1}^4 E_\theta^{\otimes i-1} \otimes \dot{E}_\theta \otimes E_\theta^{\otimes 4-i}$ can be schematically illustrated as a directed graph in Fig. 6. Each term in the summation $\sum_{i=1}^4 E_\theta^{\otimes i-1} \otimes \dot{E}_\theta \otimes E_\theta^{\otimes 4-i}$ is represented by a path from the top left vertex to the bottom right vertex.

Now we see the diagram as a matrix product in this way: each vertex represents a possible value of an index, and 2 vertices in the same column correspond to 2 possible values of an index. A directed edge from vertex i to j represents a nonzero matrix element (weight) M_{ij} . The diagram can thus be interpreted as a product of 4 matrices M_1, M_2, M_3, M_4 (our convention takes the reverse order):

$$(M_4)_{1\gamma_3} (M_3)_{\gamma_3\gamma_2} (M_2)_{\gamma_2\gamma_1} (M_1)_{\gamma_1 1}, \quad (25)$$

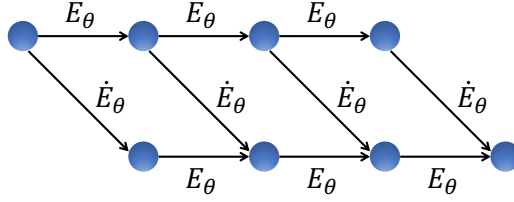


Figure 6: Matrix product diagram for expressing $dE_\theta^{\otimes 4}/d\theta$.

where each index γ_i can take two values 1 and 2. According to Fig. 6, we have

$$M_4 = \begin{pmatrix} E_\theta & \dot{E}_\theta \end{pmatrix}, \quad M_3 = M_2 = \begin{pmatrix} E_\theta & \dot{E}_\theta \\ 0 & E_\theta \end{pmatrix}, \quad M_1 = \begin{pmatrix} \dot{E}_\theta \\ E_\theta \end{pmatrix}. \quad (26)$$

Noting that each E_θ or \dot{E}_θ is regarded as a tensor with 4 indices (two α indices and two β indices) in Eq. (12), we thus complete the proof for $N = 4$. The same argument can be straightforwardly generalized to any N .

B Tensor networks for f_1 and f_2 with bounded ancilla

Apparently, if the ancilla A is accessible, one can replace \mathcal{E}_θ by $\mathcal{E}_\theta \otimes \mathcal{I}_A$ and apply the tensor contraction in Fig. 2. Nevertheless, explicitly contracting the identity operator with other tensors is unnecessary and can be safely omitted. Instead, we can make a direct connection between indices related by an identity channel.

We take the input state $\rho_0 = (\rho_0)_{\beta_1 \beta_1^a}^{\alpha_1 \alpha_1^a} |\alpha_1 \alpha_1^a \rangle \langle \beta_1 \beta_1^a|$ and the Choi operator of the i -th control operation $C_i = (C_i)_{\beta_{2i+1} \beta_{i+1}^a \beta_{2i} \beta_i^a}^{\alpha_{2i+1} \alpha_{i+1}^a \alpha_{2i} \alpha_i^a} |\alpha_{2i+1} \alpha_{i+1}^a \alpha_{2i} \alpha_i^a \rangle \langle \beta_{2i+1} \beta_{i+1}^a \beta_{2i} \beta_i^a|$, where the superscript “ a ” is associated with the ancilla and we have followed the Einstein summation convention. We then have

$$f_2 = (X^2)_{\alpha_{2N} \alpha_N^a}^{\beta_{2N} \beta_N^a} (E_\theta)_{\beta_{2N} \beta_{2N-1}}^{\alpha_{2N} \alpha_{2N-1}} (C_{N-1})_{\beta_{2N-1} \beta_N^a \beta_{2N-2} \beta_{N-1}^a}^{\alpha_{2N-1} \alpha_N^a \alpha_{2N-2} \alpha_{N-1}^a} \cdots (C_1)_{\beta_3 \beta_2^a \beta_2 \beta_1^a}^{\alpha_3 \alpha_2^a \alpha_2 \alpha_1^a} (E_\theta)_{\beta_2 \beta_1}^{\alpha_2 \alpha_1} (\rho_0)_{\beta_1 \beta_1^a}^{\alpha_1 \alpha_1^a}, \quad (27)$$

illustrated in Fig. 7(a) and

$$f_1 = X_{\alpha_{2N} \alpha_N^a}^{\beta_{2N} \beta_N^a} (M_N)_{\beta_{2N} \beta_{2N-1} \gamma_{N-1}}^{\alpha_{2N} \alpha_{2N-1}} (C_{N-1})_{\beta_{2N-1} \beta_N^a \beta_{2N-2} \beta_{N-1}^a}^{\alpha_{2N-1} \alpha_N^a \alpha_{2N-2} \alpha_{N-1}^a} \cdots (M_2)_{\beta_4 \beta_3 \gamma_2 \gamma_1}^{\alpha_4 \alpha_3} (C_1)_{\beta_3 \beta_2^a \beta_2 \beta_1^a}^{\alpha_3 \alpha_2^a \alpha_2 \alpha_1^a} (M_1)_{\beta_2 \beta_1 \gamma_1}^{\alpha_2 \alpha_1} (\rho_0)_{\beta_1 \beta_1^a}^{\alpha_1 \alpha_1^a}, \quad (28)$$

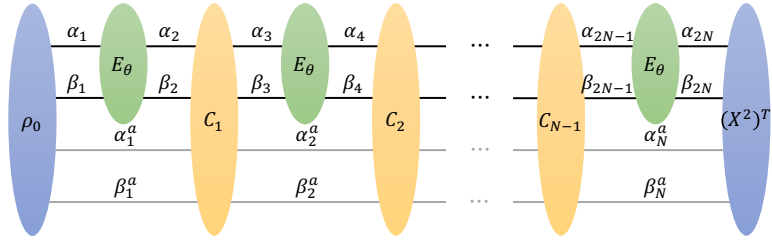
illustrated in Fig. 7(b).

C Variational circuit ansatz

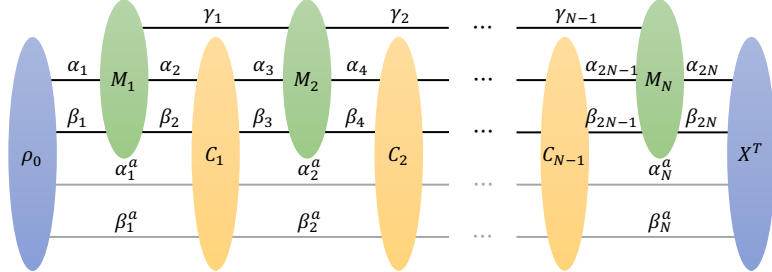
In this work we employ a simple variational ansatz $U(\phi_i)$ for the control operation C_i . For simplicity we assume that all the control operations share the same circuit layout (possibly with different parameters ϕ_i). Now we can omit the subscript and focus on one control operation $U(\phi)$.

As illustrated in Fig. 8, our ansatz for the control $U(\phi)$ consists of l layers $V_{\phi^1}, \dots, V_{\phi^l}$, and each layer comprises n single-qubit unitary gates U^3 (characterized by 3 rotational angles using the ZYZ decomposition [80]) and $n - 1$ CNOT gates connecting neighboring qubits.

In numerical experiments of estimating qubit channels, we take $n = 1, l = 1$ for the ancilla-free case and $n = 2, l = 3$ for the one-ancilla-assisted case. The variational parameters are optimized by the Adagrad algorithm [81].

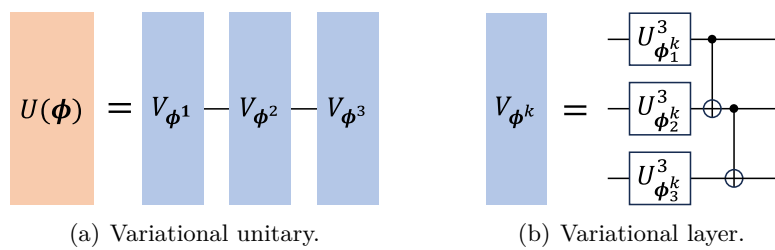


(a) Tensor network for f_2 .



(b) Tensor network for f_1 .

Figure 7: Tensor networks for computing f_2 and f_1 with bounded ancilla.



(a) Variational unitary.

(b) Variational layer.

Figure 8: Variational ansatz for $n = 3$ qubits and $l = 3$ layers.